

Double Layer Forces between Heterogeneous Charged Surfaces

S. J. Miklavic,^{*†} D. Y. C. Chan,[‡] L. R. White,[‡] and T. W. Healy[§]

Department of Mathematics and Department of Chemistry, University of Melbourne, Parkville, 3052 Victoria, Australia, and Divisions of Physical Chemistry and Food Technology, Chemical Center, University of Lund, S-221 00 Lund, Sweden

Received: March 25, 1994*

In this paper we study the double layer interaction between two heterogeneous surfaces of either constant charge or constant potential. The surface heterogeneities are assumed to be distributed on periodic lattices of arbitrary structure. General expressions for the 3-D electrostatic potential distribution and the interaction free energy between the two surfaces are given. Asymptotic forms and numerical examples for the interaction potential are provided for the symmetric lattice problem. In general, the interaction potential or osmotic pressure decays exponentially at large separations. When a nonuniform, but net neutral, surface interacts with a uniform surface (charged or uncharged), the interaction can be either attractive or repulsive depending on whether the surfaces are constant potential or constant charge. For two nonuniform net neutral surfaces, the interaction can be either attractive or repulsive depending on whether the surfaces are constrained in configurations in which regions of unlike or like charge are in opposition. For this case, a statistical mechanical average over all relative lateral displacements shows that asymptotically the interaction will *always be attractive*. The magnitude of the attraction is comparable to or can exceed the van der Waals interaction. The results given here would warrant inclusion in any interpretation of surface force measurements in systems involving adsorbing, neutralizing surfactants.

I. Introduction

A knowledge of the interaction between particles or between surfaces in general is fundamental to our understanding of many properties of colloid science. In a large class of colloidal systems, the surface forces are dominated by long-range electrostatics, the familiar double layer force.¹ For many applications under colloidal conditions the traditional approach to double layer interactions, the mean-field model based on the Poisson-Boltzmann equation, has proven to be very useful for experimental analysis. In recent years, considerable effort has gone into improving the mean-field description of the electrolyte behavior under more extreme conditions (see, for example, ref 2). In comparison, considerably less effort has been spent in studying departures from the classical assumptions which arise from a more detailed prescription of surface structure.

Techniques for scanning surface irregularities with atomic accuracy, such as atomic force microscopy (AFM), now show quite convincingly that many systems comprise surfaces which cannot be treated as uniform. In fact, there are many situations wherein nonuniformities can be envisaged to arise. In some cases this feature has been confirmed by AFM. For example, a host of these involve solutions of highly surface active species, that is, species which adsorb strongly. These species may range from polyelectrolytes, or bulky multivalent ions, of charge opposite to that of the surface to ionic amphiphiles. Our focus is on systems which possess isolated surface regions which are occupied by a concentration of charge opposite to that of the surface as for instance in the case of negatively charged mica surfaces with adsorbed or deposited cationic surfactants.³

Richmond⁴ and Nelson and McQuarrie⁵ examined the effects of discrete surface charge distributions on the double layer interaction between surfaces. From these studies one already sees that interesting and potentially important behavior can be found. While Richmond studied surfaces held at constant charge,

Kuin⁶ recently considered surfaces held at constant but nonuniform surface potential. However, Kuin's results were obtained with the superposition approximation which restricted their validity to large separations.

We recognize that it is difficult to consider a completely arbitrary charge distribution in a quantitative calculation. Consequently, we shall consider sources of charge or potential which are periodically distributed on the surface. In the next two sections we present a general formalism, outlining the process of solution of the electrostatic potential problem, and the evaluation of the interaction free energy invoking only the assumption that on each surface there is some periodic but otherwise unspecified arbitrary two-dimensional lattice distribution of charge or potential. We consider the two cases of constant charge and constant potential surfaces when the surfaces approach each other. In section IV we present numerical and asymptotic results for the interaction between two surfaces with the same periodic lattice structure. The calculations are based on distributions of inhomogeneities which are arguably more relevant than the examples given by either Richmond or Kuin. The main effect of periodic charge heterogeneities is that the additional interaction that arises can be repulsive or attractive depending on the relative transverse displacement of the surfaces. In section V, we discuss the procedure of performing the proper statistical mechanical average over possible transverse displacements of the patchy heterogeneous surfaces. The general conclusion is that when averaged over transverse displacements, the extra contribution to the interaction between from charge heterogeneities is an additional attraction between the surfaces. The paper closes with a summary of the major results.

II. Electrostatic Double Layer Potential

Consider two infinite planar half-spaces with dielectric permittivities, ϵ_1 and ϵ_3 . These are separated by a third dielectric continuum of permittivity ϵ_2 and of width h ; see Figure 1. This central medium contains a solution of simple electrolyte of species valence, z_i , in chemical equilibrium with a bulk solution of molar concentration c_{i0} , or number density, n_{i0} , at a temperature T . We are interested in determining the mean electrostatic potential,

* To whom correspondence should be addressed.

† University of Lund.

‡ Department of Mathematics, University of Melbourne.

§ Department of Chemistry, University of Melbourne.

• Abstract published in *Advance ACS Abstracts*, July 15, 1994.

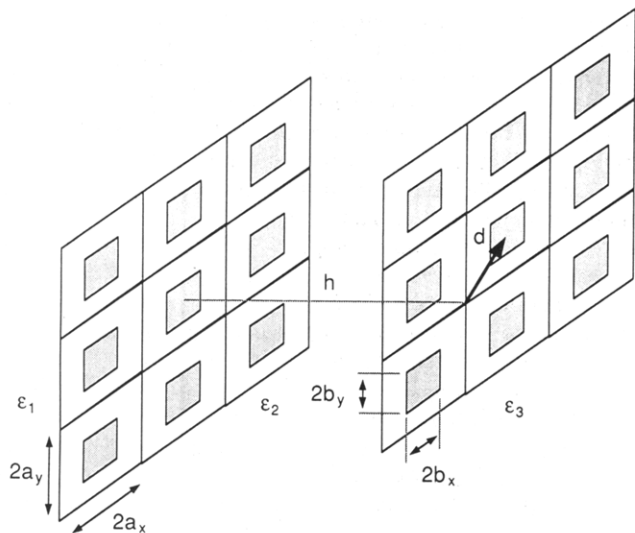


Figure 1. A schematic representation of the system under study. Two surfaces with a periodic distribution of sources of charge separated by an electrolyte solution of thickness h .

$\psi(\mathbf{r})$ across this intervening region, when the interfaces between medium 1 and 2, at $z = 0$, and between medium 2 and 3, at $z = h$, carry specified surface charge or surface potential distributions. In this paper we concentrate on either of the two limiting conditions where the surface charge or surface potential distributions are independent of separation. We shall refer to these cases as constant charge or constant potential. The intermediate cases of self-consistent regulating surfaces and the asymmetric system of one surface held at constant potential and the other held at constant charge are made the subject of a separate report.

We consider nonuniform distributions of sources $\gamma^L(\mathbf{s})$ and $\gamma^R(\mathbf{s})$ on the left and right surfaces, respectively. We use the subscripts and superscripts L or R to refer quantities to the left ($z = 0$) or right ($z = h$) interfaces, respectively. The variable γ represents either the surface potential, Ψ , or surface charge, σ , as the case may be, and $\mathbf{s} = (x, y)$ represents the transverse vector position.

Without loss of generality, we can assume that for each surface, γ contain a uniform part, γ_0 , on which is superimposed a periodic distribution of sources, γ_p . Since γ_p , and therefore γ , is periodic we may represent them by their Fourier expansions,

$$\gamma^L(\mathbf{s}) = \gamma_0^L + \sum_{\mathbf{k}_L} \gamma_{\mathbf{k}_L} \exp(i\mathbf{k}_L \cdot \mathbf{s}) \quad (1a)$$

and

$$\gamma^R(\mathbf{s}) = \gamma_0^R + \sum_{\mathbf{k}_R} \gamma_{\mathbf{k}_R} \exp(i\mathbf{k}_R \cdot \mathbf{s}) \quad (1b)$$

As stated in the Introduction, we shall not limit ourselves to the same type of lattice on each of the left and right surfaces. \mathbf{k}_L and \mathbf{k}_R therefore represent reciprocal lattice vectors for two as yet unspecified lattices. γ_0^L is in general different from γ_0^R as are the Fourier expansion coefficients, $\gamma_{\mathbf{k}_L}$ and $\gamma_{\mathbf{k}_R}$, at the same order of \mathbf{k}_L and \mathbf{k}_R . These coefficients can be obtained once a prescription for $\gamma^L(\mathbf{s})$ and $\gamma^R(\mathbf{s})$ in real space is given. Notably, they are obtained from the Fourier inversion theorem,

$$\gamma_{\mathbf{k}_j} = \frac{1}{A_j} \int_{A_j} (\gamma^j(\mathbf{s}) - \gamma_0^j) \exp(-i\mathbf{k} \cdot \mathbf{s}) \, ds \quad (2)$$

where A_j is the area of the unit cell on the $j = L$ or R lattice. We note that the $\mathbf{k} = 0$ term of the expansion also contributes to the uniform background, according to (2), with an *area average* of the periodic part.

For an arbitrary electrolyte the electrostatic potential, $\psi(\mathbf{r})$, satisfies the following equations

$$\nabla^2 \psi(\mathbf{r}) = 0 \quad \text{for } z < 0, z > h \quad (3a)$$

$$\nabla^2 \psi(\mathbf{r}) = -\frac{4\pi}{\epsilon_2} \rho(\mathbf{r}) \quad \text{for } 0 < z < h \quad (3b)$$

with volume charge density, $\rho(\mathbf{r})$ at \mathbf{r} given by ($\beta = 1/k_B T$)

$$\rho(\mathbf{r}) = \sum_i z_i e n_{i0} \exp(-z_i e \beta \psi(\mathbf{r})) \quad (4)$$

Since the surface source distributions are no longer uniform, the scalar mean potential retains its dependence on the three-dimensional vector position, \mathbf{r} , and the equations to be solved are partial differential equations. A simplifying assumption that can often be made is to assume that $\psi(\mathbf{r})$ is small everywhere, i.e., $e\psi(\mathbf{r})/k_B T < 1$; we may then linearize the dependence of the ionic densities on the mean potential to give

$$\rho(\mathbf{r}) = -\sum_i z_i^2 e^2 n_{i0} \beta \psi(\mathbf{r}) \quad (5)$$

Note that this approximation is better for symmetric electrolytes as the $O(\psi^2)$ term in the expansion vanishes identically. Basically, the linearization assumption is needed to achieve any analytical progress. However, what qualitative features appear in the linearized model are certain to remain in the more complex nonlinear calculation. The approximation we adopt therefore does not detract from our conclusions. Given the form of the source functions on the boundaries, together with the linearity of the problem, the solution for the electrostatic potential $\psi(\mathbf{r})$ can be expressed as a Fourier expansion in terms of the transverse coordinates $\mathbf{s} = (x, y)$

$$\psi(\mathbf{r}) = \sum_{\mathbf{k}_L} \varphi_{\mathbf{k}_L}(z) \exp(i\mathbf{k}_L \cdot \mathbf{s}) + \sum_{\mathbf{k}_R} \varphi_{\mathbf{k}_R}(z) \exp(i\mathbf{k}_R \cdot \mathbf{s}) \quad (6)$$

where the Fourier coefficients, $\varphi_{\mathbf{k}}(z)$, depend on the wave vector \mathbf{k} and the normal coordinate z .

Substitution of (6) into (3) gives a set of four ordinary differential equations for each \mathbf{k} :

$$\varphi_{\mathbf{k}_j}''(z) - k_j^2 \varphi_{\mathbf{k}_j}(z) = 0 \quad \text{for } z < 0, z > h \quad (7a)$$

$$\varphi_{\mathbf{k}_j}''(z) - q_j^2 \varphi_{\mathbf{k}_j}(z) = 0 \quad \text{for } 0 < z < h \quad (7b)$$

for $j = L, R$, where $q_j = [(\kappa^2 + k_j^2)]^{1/2}$, and the usual inverse Debye length is $\kappa = [(4\pi e^2 \beta / \epsilon_2) \sum_i z_i^2 n_{i0}]^{1/2}$. Solutions of these differential equations which remain finite for all values of z are

$$\varphi_{\mathbf{k}_j}(z) = A(k_j) \exp(k_j z) \quad z < 0 \quad (8a)$$

$$\varphi_{\mathbf{k}_j}(z) = B(k_j) \exp(q_j z) + C(k_j) \exp(-q_j z) \quad 0 < z < h \quad (8b)$$

$$\varphi_{\mathbf{k}_j}(z) = D(k_j) \exp(-k_j z) \quad z > h \quad (8c)$$

for $j = L, R$, where the coefficients A, B, C , and D have to be chosen to satisfy appropriate boundary conditions.

As we have two linearly independent expansions in (6), which individually are appropriate expansions to accommodate the boundary conditions to be satisfied on one of the two surfaces, we only need to impose constraints on each solution on the other surface. For instance, the expansion given by the first series in (6) can be made to satisfy the boundary conditions on the left-hand surface at $z = 0$, so the condition on the second series is that it should vanish at $z = 0$. Likewise, the first series should vanish

at the right-hand surface at $z = h$ since the expansion given by the second series in (6) can be made to satisfy the conditions at $z = h$. Explicitly, if the surfaces are held at constant potential, where $\gamma(s) = \Psi(s)$ is a given function, then the appropriate set of conditions on the Fourier coefficients are that

$$\varphi_{k_L}(0) = \Psi_{k_L} \quad \varphi_{k_L}(h) = 0 \quad (9a)$$

$$\varphi_{k_R}(0) = 0 \quad \varphi_{k_R}(h) = \Psi_{k_R} \quad (9b)$$

where Ψ_{k_L} and Ψ_{k_R} are the known Fourier coefficients in the series representation for the specified surface potential distribution, $\Psi(s)$, on each surface. On the other hand, if the surfaces are held at constant charge, where $\gamma(s) = \sigma(s)$ is a given function, then the boundary conditions are that the potential and the normal component of the displacement field be continuous across the interface

$$\epsilon_2 \varphi'_{k_L}(0^+) - \epsilon_1 \varphi'_{k_L}(0^-) = -4\pi \sigma_{k_L};$$

$$\epsilon_2 \varphi'_{k_L}(h^-) = \epsilon_3 \varphi'_{k_L}(h^+) \quad (10a)$$

$$\epsilon_1 \varphi'_{k_R}(0^-) = \epsilon_2 \varphi'_{k_R}(0^+);$$

$$\epsilon_3 \varphi'_{k_R}(h^+) - \epsilon_2 \varphi'_{k_R}(h^-) = -4\pi \sigma_{k_R} \quad (10b)$$

where σ_{k_L} and σ_{k_R} are the known Fourier coefficients in the series representation for the specified surface charge distribution, $\sigma(s)$ on each surface.

For the constant potential case, only the solution for φ_{k_L} in $0 \leq z \leq h$ are required and they are

$$\varphi_{k_L}(z) = \Psi_{k_L} \frac{\sinh(q_L(h-z))}{\sinh(q_L h)} \quad \varphi_{k_R}(z) = \Psi_{k_R} \frac{\sinh(q_R z)}{\sinh(q_R h)} \quad (11)$$

For surfaces held at constant charge, the solutions for z between 0 and h are dependent on the solutions outside the central region: $z < 0$ and $z > h$. This arises from the effect of ion image interactions introduced by the dielectric discontinuities. In general, the solutions (8) for $0 \leq z \leq h$ satisfying eqs 10 are

$$\varphi_{k_L}(z) = \frac{4\pi}{\mathcal{N}_L} \frac{\sigma_{k_L} e^{-q_L h}}{\epsilon_2 q_L + \epsilon_1 k_L} (\Delta_{23}^L e^{q_L(z-h)} + e^{-q_L(z-h)}) \quad (12a)$$

$$\varphi_{k_R}(z) = \frac{4\pi}{\mathcal{N}_R} \frac{\sigma_{k_R} e^{-q_R h}}{\epsilon_2 q_R + \epsilon_3 k_R} (e^{q_R z} + \Delta_{21}^R e^{-q_R z}) \quad (12b)$$

where

$$\mathcal{N}_j = 1 - \Delta_{21}^j \Delta_{23}^j \exp(-2q_j h) \quad j = L, R \quad (13)$$

and the ratio

$$\Delta_{2i}^j = \frac{\epsilon_2 q_j - \epsilon_i k_j}{\epsilon_2 q_j + \epsilon_i k_j} \quad j = L, R; i = 1, 3 \quad (14)$$

is a measure of the strength of dielectric images on the left and right side. By inserting either eqs 11, for constant potential surfaces, or eqs 12, for constant charge, into the double Fourier expansion for $\psi(r)$ in eq 6, one can obtain all the necessary information to evaluate any thermodynamic property of the electrical double layer. Also, the splitting of the terms as given by either eqs 11 or 12 naturally highlights the direct contributions from either surface to the total potential at a given position z .

However, in each case there is always an indirect contribution which recognizes the presence of the other surface, represented by the term in the denominators of (11) and (12) which depends on the separation h . In the case of constant surface charge the dielectric discontinuities also contribute. Consequently, despite the linearity of the problem, our solutions are not to be confused with a superposition approximation, in which the important factors in the denominator of (11) and (12), and the factors, Δ_{2i} , which are explicit in eqs 12 do not appear. We point out that eqs 12 represent the generalization of expressions obtained by Richmond⁴ for symmetric lattices, to the case of arbitrary lattices. For the special case of symmetric lattices, our expressions for constant potential surfaces therefore remain the complete solution to this problem attempted by Kuin⁶ who in fact invoked the superposition approximation, using the mean potential for an isolated surface.

In the case of surfaces held at constant potential, the corresponding values of surface charge are obtained by evaluating the derivative of the potential at the respective surfaces. That is,

$$\sigma^L(s) = -\frac{\epsilon_2}{4\pi} \frac{d\psi(s;0)}{dz} \quad \sigma^R(s) = \frac{\epsilon_2}{4\pi} \frac{d\psi(s;h)}{dz} \quad (15)$$

These results are needed for the calculation of surface and double layer free energies discussed in the next section.

III. Double Layer Interaction Free Energy

The free energy of the double layer can be obtained by a thermodynamic charging integration,^{1,4,7,8} which depends on the assumed surface equation of state. In the linear theory, the expression for the free energy per unit area is simply

$$F(h) = \pm \frac{1}{2A} \int_A \int_A \sigma(s)\psi(s) ds \quad (16)$$

where the negative or positive sign is taken appropriately for surfaces at constant potential or constant charge. Naturally, as each surface has a nonuniform source distribution, one must perform an area average over the surfaces at $z = 0$ and at $z = h$. Kuin⁶ indicated no such average in his evaluation of the double layer free energy. Quite simply, the integral over A separates into two contributions, one for each surface, which we shall denote by F^L and F^R . The values of surface potential and charge appearing in eqs 16 are taken from the respective cases given in the previous section. For surfaces interacting at constant potential, $\gamma = \Psi$ is prescribed on each surface—the first of eqs 1 appears in F^L and the second in F^R . The corresponding surface charge densities, σ are found from (15) using (6) and (11). Performing the operations indicated in eq 15 and substituting into (16) above, we have

$$F^L(h) = -\frac{\epsilon_2}{8\pi A} \int_A \int_A ds \sum_{k_L} \Psi_{k_L} e^{ik_L \cdot s} \left[\sum_{k'_L} q'_L \Psi_{k'_L} \coth(q'_L h) e^{ik'_L \cdot s} - \sum_{k_R} \frac{q_R \Psi_{k_R} e^{ik_R \cdot s}}{\sinh(q_R h)} \right] \quad (17)$$

For periodic functions, the integral over A breaks down into an integral over the unit cell, in this case A_L for the left surface, multiplied by the number of unit cells within A . Evaluating the

integral, we find

$$F^L(h) = -\frac{\epsilon_2}{8\pi} \sum_{\mathbf{k}_L} q_L \Psi_{\mathbf{k}_L} \Psi_{-\mathbf{k}_L} \coth(q_L h) + \frac{\epsilon_2}{8\pi} \sum_{\mathbf{k}_L} \sum_{\mathbf{k}_R} \frac{q_R \Psi_{\mathbf{k}_R} \Psi_{\mathbf{k}_L}}{\sinh(q_R h)} C_L(\mathbf{k}_L, \mathbf{k}_R) \quad (18)$$

where we have used the fact that, as \mathbf{k}_L and \mathbf{k}'_L are reciprocal lattice vectors of the lattice at $z = 0$, we have the identity

$$\frac{1}{A_L} \int_{A_L} \exp(i(\mathbf{k}_L + \mathbf{k}'_L) \cdot \mathbf{s}) \, ds = \delta_{\mathbf{k}'_L, -\mathbf{k}_L} = 1 \quad \text{if } \mathbf{k}'_L = -\mathbf{k}_L \quad (19)$$

$$= 0 \quad \text{otherwise}$$

We have also introduced the quantity

$$C_L(\mathbf{k}_L, \mathbf{k}_R) = \frac{1}{A_L} \int_{A_L} \exp(i(\mathbf{k}_L + \mathbf{k}_R) \cdot \mathbf{s}) \, ds \quad (20)$$

with the integral evaluated over a unit cell A_L . A similar expression for F^R can be obtained directly from symmetry. The result is

$$F^R(h) = -\frac{\epsilon_2}{8\pi} \sum_{\mathbf{k}_R} q_R \Psi_{\mathbf{k}_R} \Psi_{-\mathbf{k}_R} \coth(q_R h) + \frac{\epsilon_2}{8\pi} \sum_{\mathbf{k}_L} \sum_{\mathbf{k}_R} \frac{q_R \Psi_{\mathbf{k}_R} \Psi_{\mathbf{k}_L}}{\sinh(q_L h)} C_R(\mathbf{k}_L, \mathbf{k}_R) \quad (21)$$

where

$$C_R(\mathbf{k}_L, \mathbf{k}_R) = \frac{1}{A_R} \int_{A_R} \exp(i(\mathbf{k}_L + \mathbf{k}_R) \cdot \mathbf{s}) \, ds \quad (22)$$

For a general discussion, the lattices, L and R, are treated as dissimilar; therefore, the reciprocal lattice of the left surface, \mathbf{k}_R cannot, in general, be expressed as a simple combination of basis vectors of, \mathbf{k}_L , the reciprocal lattice of the left surface; thus, C_L is nontrivial. When the lattices L and R are identical, C_R and C_L reduce to a Kronecker delta function, as in (19). We remark that in deriving (18) and (21) we have used the fact that $q_{L,R} = [(\kappa^2 + k_{L,R}^2)]^{1/2}$ is invariant under a sign change of $\mathbf{k}_{L,R}$.

For the free energy of surfaces held at constant charge: $\gamma = \sigma$ is prescribed on each surface and ψ is given by expansion (6) with coefficients (12). The free energy again separates into two contributions, F^L and F^R . $F^L(h)$ is given by

$$F^L(h) = \frac{1}{2} \sum_{\mathbf{k}_L} \sigma_{\mathbf{k}_L} \varphi_{-\mathbf{k}_L}(0) + \frac{1}{2} \sum_{\mathbf{k}_L} \sum_{\mathbf{k}_R} \sigma_{\mathbf{k}_L} \varphi_{\mathbf{k}_R}(0) C_L(\mathbf{k}_L, \mathbf{k}_R) \quad (23)$$

To obtain this result we have argued as before: because of periodicity, the integral over A is equivalent to an integral over the unit cell multiplied by the number of unit cells in A . C_L is given by (20). $F^R(h)$ can be deduced from symmetry, $L \rightarrow R$, $z = 0 \rightarrow z = h$

$$F^R(h) = \frac{1}{2} \sum_{\mathbf{k}_R} \sigma_{\mathbf{k}_R} \varphi_{-\mathbf{k}_R}(h) + \frac{1}{2} \sum_{\mathbf{k}_L} \sum_{\mathbf{k}_R} \sigma_{\mathbf{k}_R} \varphi_{\mathbf{k}_L}(h) C_R(\mathbf{k}_L, \mathbf{k}_R) \quad (24)$$

Inserting the coefficients φ_k of (12) we obtain the following results

which show the explicit dependence on separation, h ,

$$F^L(h) = 2\pi \sum_{\mathbf{k}_L} \sigma_{\mathbf{k}_L} \left[\frac{\sigma_{-\mathbf{k}_L} (1 + \Delta_{23}^L e^{-2q_L h})}{\mathcal{N}_L(\epsilon_2 q_L + \epsilon_1 k_L)} + \sum_{\mathbf{k}_R} \frac{\sigma_{\mathbf{k}_R} e^{-q_R h} (1 + \Delta_{21}^R)}{\mathcal{N}_R(\epsilon_2 q_R + \epsilon_3 k_R)} C_L(\mathbf{k}_L, \mathbf{k}_R) \right] \quad (25)$$

and

$$F^R(h) = 2\pi \sum_{\mathbf{k}_R} \sigma_{\mathbf{k}_R} \left[\frac{\sigma_{-\mathbf{k}_R} (1 + \Delta_{21}^R e^{-2q^R h})}{\mathcal{N}_R(\epsilon_2 q_R + \epsilon_3 k_R)} + \sum_{\mathbf{k}_L} \frac{\sigma_{\mathbf{k}_L} e^{-q_L h} (1 + \Delta_{23}^L)}{\mathcal{N}_L(\epsilon_2 q_L + \epsilon_1 k_L)} C_R(\mathbf{k}_L, \mathbf{k}_R) \right] \quad (26)$$

To obtain the interaction free energy, $V(h)$, one takes the difference between F at finite h and F evaluated at infinite separation. That is,

$$V(h) = F(h) - F(\infty) \quad (27)$$

where, for constant potential surfaces

$$F(\infty) = -\frac{\epsilon_2}{8\pi} \sum_{\mathbf{k}_L} q_L \Psi_{\mathbf{k}_L} \Psi_{-\mathbf{k}_L} - \frac{\epsilon_2}{8\pi} \sum_{\mathbf{k}_R} q_R \Psi_{\mathbf{k}_R} \Psi_{-\mathbf{k}_R} \quad (28)$$

and, for constant charge surfaces,

$$F(\infty) = 2\pi \sum_{\mathbf{k}_L} \left[\frac{\sigma_{\mathbf{k}_L} \sigma_{-\mathbf{k}_L}}{(\epsilon_2 q_L + \epsilon_1 k_L)} \right] + 2\pi \sum_{\mathbf{k}_R} \left[\frac{\sigma_{\mathbf{k}_R} \sigma_{-\mathbf{k}_R}}{(\epsilon_2 q_R + \epsilon_3 k_R)} \right] \quad (29)$$

IV. Numerical and Asymptotic Results for Similar Lattices

The general solution presented in the preceding sections contains a large number of parameters. For our numerical study, we consider two surfaces with identical lattice structure, but retaining the option of dissimilar source values, γ_0 and γ_p . That is, the lattices have now the same lattice structure, but the periodic potential/charge amplitude may be different. A study of dissimilar lattices will be considered elsewhere.

We first derive and discuss some general results that apply to surfaces with identical lattice structures. We shall then give results for a specific type of lattice. For identical lattices, the reciprocal lattice vectors, \mathbf{k} , and the areas of the unit cells are identical.

$$\mathbf{k}_L = \mathbf{k}_R, \quad q_L = q_R, \quad A_L = A_R$$

Similar reduction occurs in eqs 13 and 14. Consequently, the two expansion sets in (1) become identical and the two sums in (6) merge into one. The values for the C functions also simplify in the case of identical lattices,

$$C_L(\mathbf{k}_L, \mathbf{k}_R) = C_R(\mathbf{k}_L, \mathbf{k}_R) = 1 \quad \text{if } \mathbf{k}_R = -\mathbf{k}_L$$

$$= 0 \quad \text{otherwise}$$

which leaves us with quite simple expressions for our principal results, namely the interaction free energies. Hereafter, we can also drop the L and R subscripts on the wave vector since $\mathbf{k}_L = \mathbf{k}_R$. Finally then, for surfaces with identical lattice structures,

held at constant potential, the interaction free energy is

$$V^p(h) = \frac{\epsilon_2}{8\pi} \sum_{\mathbf{k}} \frac{q}{\sinh(qh)} [(\Psi_{-\mathbf{k}}^L \Psi_{\mathbf{k}}^R + \Psi_{-\mathbf{k}}^R \Psi_{\mathbf{k}}^L) \cos(\mathbf{k} \cdot \mathbf{d}) - (\Psi_{-\mathbf{k}}^L \Psi_{\mathbf{k}}^L + \Psi_{-\mathbf{k}}^R \Psi_{\mathbf{k}}^R) e^{-qh}] \quad (30)$$

and, for constant charge surfaces, the interaction free energy is given by

$$V^c(h) = 4\pi \sum_{\mathbf{k}} \frac{\epsilon_2 q e^{-qh}}{\mathcal{N}} \left[\frac{(\sigma_{-\mathbf{k}}^L \sigma_{\mathbf{k}}^R + \sigma_{-\mathbf{k}}^R \sigma_{\mathbf{k}}^L) \cos(\mathbf{k} \cdot \mathbf{d})}{(\epsilon_2 q + \epsilon_1 k)(\epsilon_2 q + \epsilon_3 k)} + \left(\frac{\sigma_{-\mathbf{k}}^L \sigma_{\mathbf{k}}^L \Delta_{23}}{(\epsilon_2 q + \epsilon_1 k)^2} + \frac{\sigma_{-\mathbf{k}}^R \sigma_{\mathbf{k}}^R \Delta_{21}}{(\epsilon_2 q + \epsilon_3 k)^2} \right) e^{-qh} \right] \quad (31)$$

We have introduced the phase factor, $\cos(\mathbf{k} \cdot \mathbf{d})$, which originates from the Fourier coefficients, $\gamma_{\mathbf{k}\alpha}$, of expansion 1b. This factor allows the lattices to be displaced laterally relative to one another by a vectorial amount $\mathbf{d} = (d_x, d_y)$, written in Cartesian coordinates. We again point out that (31) is identical to Richmond's eq 4.3 in ref 4 and reduces to his eq 23 in ref 4b when $\epsilon_1 = \epsilon_3$. It is of interest to determine the asymptotic forms of eqs 30 and 31. These will help in the interpretation of numerical results and are potentially useful for direct experimental analysis. Each term in the sum in (30) and (31) decays exponentially with separation, h . Naturally, as h becomes very large, the interaction quickly becomes dominated by the term with the smallest value of $k = |\mathbf{k}|$. For surfaces with a net nonzero surface charge, this smallest value is $\mathbf{k} = \mathbf{0}$ which corresponds to the standard uniform double layer result: the force decays exponentially with decay length given by κ^{-1} . However, for the systems that are exactly "neutralized" by adsorbed counterionic species, the zero k term vanishes, by construction. These surfaces contain periodic positive and negative regions which, while locally charged, are neutral when averaged over a unit cell. The interaction for large h is then determined by the next lowest terms in the expansion, terms corresponding to the smallest nonzero value of $k = k_{\min}$ with $q_{\min} = [(\kappa^2 + k_{\min}^2)]^{1/2}$. For identical, net neutral surfaces, at constant potential the asymptotic form of the interaction free energy is then

$$V^p(h) = \frac{\epsilon_2 q_{\min}}{4\pi} [(\Psi_{-\mathbf{k}}^L \Psi_{\mathbf{k}}^R + \Psi_{-\mathbf{k}}^R \Psi_{\mathbf{k}}^L) \cos(\mathbf{k} \cdot \mathbf{d})]_{k=k_{\min}} \times \exp(-q_{\min} h) \quad (32)$$

while, for constant charge surfaces, the interaction potential is given by

$$V^c(h) = 4\pi \epsilon_2 q_{\min} \left[\frac{(\sigma_{-\mathbf{k}}^L \sigma_{\mathbf{k}}^R + \sigma_{-\mathbf{k}}^R \sigma_{\mathbf{k}}^L) \cos(\mathbf{k} \cdot \mathbf{d})}{(\epsilon_2 q + \epsilon_1 k)(\epsilon_2 q + \epsilon_3 k)} \right]_{k=k_{\min}} \times \exp(-q_{\min} h) \quad (33)$$

If there are several wave vectors with the same magnitude, k_{\min} , that is if k_{\min} is degenerate, then all terms with the same k_{\min} will contribute to the asymptotic behavior, each represented by expressions like the formulas above.

We shall now consider the interaction between surfaces that are net neutral but contain charged patches that are distributed periodically on the surface. For such systems, there are three important observations to be deduced from the last two equations. Firstly, there is the obvious fact that a net interaction exists with magnitude governed by the strength of the periodically distributed sources. The underlying uniform surface charge does not play

any role here apart from providing a charge that exactly neutralizes the periodic charges distribution. Secondly, the force decays exponentially with decay length $1/q_{\min}$ rather than $1/\kappa$. Our understanding of double layer interactions must now be modified to take into account the competition between the usual decay length scale of κ^{-1} which is associated with electrical double layer interaction between charged surfaces and another decay length scale, k_{\min}^{-1} , introduced by the discreteness of the lattice of charged patches. When the salt content becomes sufficiently high so that κ is large compared to k_{\min} , the discreteness of the lattice is unimportant and the force decays as we expect. The interesting cases are therefore those with low salt content, $\kappa \ll k_{\min}$, for which we will see the lattice dimension being reflected in the characteristic length of the double layer interaction that arises out of the presence of charged patches.

Finally, for surfaces with the same lattice symmetry, because of the phase factor, $\cos(\mathbf{k} \cdot \mathbf{d})$, the interaction for both the constant potential and constant charge cases can be either repulsive or attractive. When the two lattices are in register, that is, when the relative displacement vector $\mathbf{d} = \mathbf{0}$, the repulsive force is a maximum. When the surfaces are exactly out of register, that is, $\mathbf{k} \cdot \mathbf{d} = \pi$, so that $\cos(\mathbf{k} \cdot \mathbf{d}) = -1$, the attractive force is maximal. However, for asymmetric cases, when the sources on one surface are of opposite sign to the sources on the other, which implies that the underlying uniform charges are also of opposite sign, the dependence on the phase is the reverse: the attractive force is greatest when the surfaces are in register and the repulsive force is greatest when the surfaces are exactly out of register. This is not difficult to appreciate. The lowest (highest) energy configuration, that is, attraction (repulsion), corresponds to the situation when regions of unlike (like) sign are in opposition.

Further interesting features appear when we consider what happens when a net neutral patchy surface (the left surface L, say), in the above sense, interacts with a uniformly charged nonpatchy surface (the right surface R, say), that is, when $\gamma_p^R = 0$. The asymptotic forms for this case are easily deduced from eqs 30 and 31. When the uniform surface is charged, the magnitude of the interaction is governed by its source value. For constant potential surfaces, we have for the interaction free energy

$$V^p(h) = -\frac{\epsilon_2 \kappa}{4\pi} \Psi_0^R \Psi_0^R \exp(-2\kappa h) \quad (34a)$$

while, for constant charge surfaces, we have

$$V^c(h) = 4\pi \frac{\sigma_0^R \sigma_0^R}{\epsilon_2 \kappa} \exp(-2\kappa h) \quad (35a)$$

As should be expected, this pair of expressions is independent of the phase variable, \mathbf{d} . From these asymptotic forms we see that the constant potential interaction is *always attractive* while the constant charge interaction is *always repulsive*. The interaction decays exponentially with characteristic length one-half of the usual Debye length, κ^{-1} .

When the *uniform* surface is *uncharged*, that is, electrically neutral, so that $\gamma_0^R = \gamma_p^R = 0$, then the interaction free energy is

$$V^p(h) = -\frac{\epsilon_2 q_{\min}}{4\pi} \Psi_{-\mathbf{k}_{\min}}^L \Psi_{\mathbf{k}_{\min}}^L \exp(-2q_{\min} h) \quad (34b)$$

for a constant potential net neutral patchy surface interacting with an uncharged surface, and

$$V^c(h) = 4\pi \epsilon_2 q_{\min} \frac{\sigma_{-\mathbf{k}_{\min}}^L \sigma_{\mathbf{k}_{\min}}^L \Delta_{23}}{(\epsilon_2 q_{\min} + \epsilon_1 k_{\min})^2} \exp(-2q_{\min} h) \quad (35b)$$

for a constant charge net neutral patchy surface interacting with an uncharged surface. As in the symmetric case the value of k_{\min}

may be degenerate. The magnitude is now dependent on the value of the periodically distributed source on the net neutral patchy surface. The force also decays exponentially but with characteristic length one-half the value obtained in the symmetric problem (cf., eqs 32 and 33). That the forces are attractive and repulsive, respectively, for constant potential and constant charge conditions of dissimilar, uniform surfaces has been known for some time. Evidently, these same conditions continue up through the higher order modes of the Fourier expansion, as an examination of eqs 30 and 31 will show.

This completes our survey of general results for the interaction between patchy surfaces with identical lattice structures or between a patchy surface and an uncharged surface. For our numerical study, we have selected rectangular lattices on both surfaces. We place our origin at the center of a cell which extends over the ranges $-a_x \leq x \leq a_x$ and $-a_y \leq y \leq a_y$. In a Cartesian coordinate system the appropriate real lattice vector is $\mathbf{a} = n(2a_x, 0) + m(0, 2a_y)$ and the reciprocal lattice vector is then $\mathbf{k} = n(\pi/a_x, 0) + m(0, \pi/a_y)$, where m and n run over all positive and negative integers. In general, a_x does not necessarily equal to a_y , although for most of the case studies we have set $a_x = a_y = 100 \text{ \AA}$. The area of the unit cell is then $A = 4a_x a_y$. As pointed out earlier, the interesting cases are at low ionic strength where the decay of the interaction free energy is controlled by the lattice spacing of the charged patches. We have therefore focused on a monovalent electrolyte at a concentration of $2.25 \times 10^{-5} \text{ M}$, which gives a Debye length of $\kappa^{-1} = 640.7 \text{ \AA}$. Other variables are $T = 298 \text{ K}$, $\epsilon_2 = 78.5$, and $\epsilon_1 = \epsilon_3$ are set to be either 78.5 or 2, as the two extreme values.

To model experimentally realizable conditions we have chosen to represent the periodically distributed sources as finite-sized rectangular regions, rather than point charges^{4,5} or continuous functions.⁶ Centered within each rectangular unit cell is a rectangular "patch" of area $B = 4b_x b_y$; obviously we must have $b_x \leq a_x$ and $b_y \leq a_y$ (see Figure 1). Within a unit cell then, a patch occupies the region $-b_x \leq x \leq b_x$ and $-b_y \leq y \leq b_y$, and so our source functions, $\gamma(\mathbf{s})$, of eq 1 can be written as

$$\gamma^j(\mathbf{s}) = \gamma_p^j \theta(x + b_x) \theta(b_x - x) \theta(y + b_y) \theta(b_y - y) + \gamma_0^j \quad (36)$$

where $j = \text{L, R}$, $\mathbf{s} = (x, y)$, γ_p^j is a constant that specifies the strength of the source, and

$$\theta(x) = \begin{cases} 0 & x < 0 \\ 1 & x > 0 \end{cases} \quad (37)$$

is the Heaviside step function. With this representation, the Fourier coefficients are straightforward to determine. Elementary integration gives

$$\gamma_k^j = \frac{\gamma_p^j 4 \sin(k_x b_x) \sin(k_y b_y)}{A k_x k_y} \quad (38)$$

This functional form is the same for both surfaces, $j = \text{L, R}$. The $k = 0$ term of the expansion now includes a sum of two terms—a contribution from the uniform background source γ_0 , and an area-weighted contribution according to the relative areas of the unit cell, A , and the area of the patch area, B , which arises from the patch distribution

$$U_0^j = \gamma_0^j + (B/A) \gamma_p^j \quad (39)$$

In most of the numerical case studies, we focus on conditions in which this uniform value is zero, that is, $U_0 = 0$, which corresponds to a net neutral patchy surface. This can be achieved by manipulating the six parameters, a_x , a_y , b_x , b_y , γ_p^j , and γ_0^j , implicitly present in (39), in a variety of interdependent combinations. Although of intrinsic interest, we do not consider

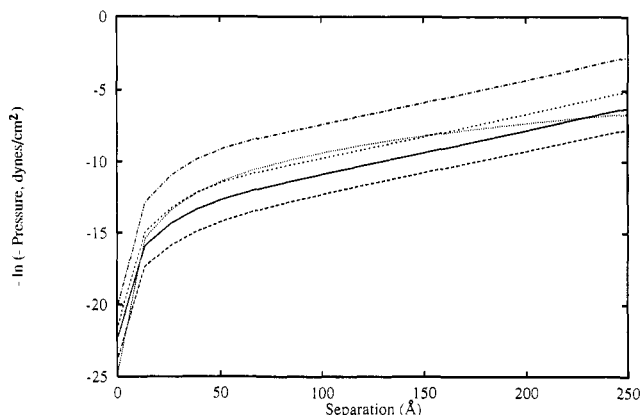


Figure 2. Pressure vs surface separation for constant potential surfaces, plotted on natural logarithmic scale. The underlying surface potential was kept fixed at -50 mV or $2 kT/e$. The potential on the square patches were adjusted together with the size of the patch, $4b^2$, to satisfy the constraint $U_0 = 0$. In order of increasing attraction, the potential values are 2.22, 2.77, 3.56, and $8 kT/e$. The unit cell parameters are $a_x = a_y = 100 \text{ \AA}$ and $\cos(\mathbf{k} \cdot \mathbf{d}) = -1$. The salt concentration was kept fixed at $2.5 \times 10^{-5} \text{ M}$. The van der Waals interaction using a Hamaker constant of $2.2 \times 10^{-20} \text{ J}$ is given by the dotted line.

the asymmetric case where both surfaces are neutral but with a different combination of these parameters.

We shall mainly present results for the disjoining pressure, $P(h)$. For the most part, the disjoining pressure, $P(h)$, and the interaction free energy per unit area, $V(h)$, are very similar in their quantitative dependence on separation, and only where there are noticeable differences do we present both. The disjoining pressure is found by taking the negative derivative of V or F with respect to separation. This is straightforward to do using eqs 30 and 31. To within a factor of 2π , $P(h)$ represents the gradient of the force between crossed cylinders (normalized by their average radius) in surface force experiments⁹ and is therefore also of experimental interest.

To get an idea of the magnitudes of the attractive forces one can obtain, we include in Figure 2 the van der Waals force per unit area, $-A/6\pi h^3$. Where we have used a Hamaker constant of $A = 2.2 \times 10^{-20} \text{ J}$ which is appropriate for two mica surfaces interacting across water. With this we compare the exponentially decaying attractive forces between constant potential surfaces, each given a uniform background value of -50 mV , with the distributed potential regions adjusted in area and strength to ensure that the surface is net neutral, that is, $U_0 = 0$, at infinite separation. The unit cell is kept fixed with $a_x = a_y = 100 \text{ \AA}$, and the two lattices are displaced relative to one another by half a unit cell so that $\cos(\mathbf{k} \cdot \mathbf{d}) = -1$. The different curves in Figure 2, in order of diminishing magnitude, refer to increasing size of the charged patches. It is clear from the force curves shown, with patch potentials starting at about 70 mV , that these attractive double layer forces can be large compared with the van der Waals force over a substantial separation range. Because these double layer forces are exponentially decaying, the van der Waals power law dominate at sufficiently large separations. It is obvious from the electroneutrality condition, $U_0 = 0$, together with the fact that these forces are determined by the magnitude of the patch strength, that the greater the background potential, the more will these forces exceed van der Waals. It is interesting to compare these curves with, say, the experimental results of Pashley et al.,³ on forces between adsorbed CTAB surfaces.

A clear feature of the curves is that two functional dependences on separation are evident, namely exponential at large distances and a power law at small separations. However, on a logarithmic plot, one may be tempted to fit the observed behavior with two exponential functions of different decay lengths. This is in fact routinely done on measured "hydration" force curves. We may determine graphically that the slopes of these lines correspond

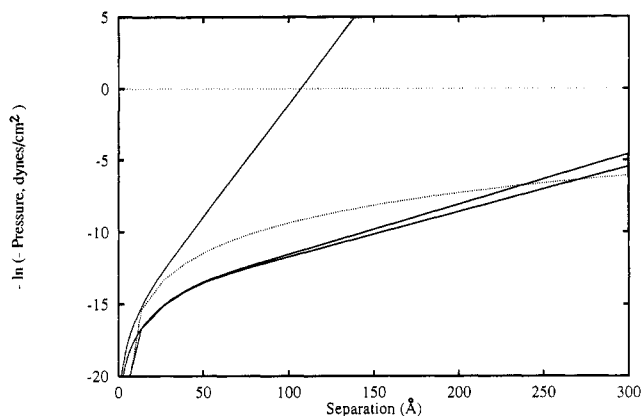


Figure 3. Pressure vs surface separation for constant potential surfaces, plotted on natural logarithmic scale. The underlying surface potential was kept fixed at -75 mV or $3 kT/e$ and the potential on the patches was $5.33 kT/e$. The lattice parameters are $a_x = a_y = 100$ Å and $\cos(\mathbf{k}\cdot\mathbf{d}) = -1$. Three salt concentrations are shown in order of increasing attraction 0.25 , 2.5×10^{-3} , and 2.5×10^{-2} M. The van der Waals interaction using a Hamaker constant of 2.2×10^{-20} J is given by the dotted line.

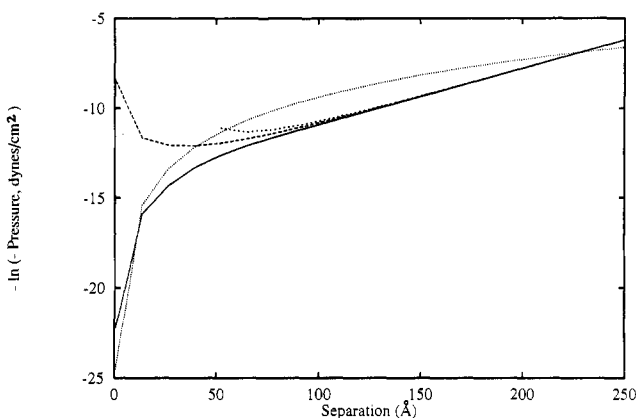


Figure 4. Pressure vs surface separation for constant potential surfaces (solid line), constant charge with no dielectric discontinuities (long dashed line), and constant charge with dielectric discontinuities, $\epsilon_1 = \epsilon_3 = 2$ (short dashed line). The underlying surface potential was kept fixed at -50 mV or $2kT/e$ and the potential on the patches was $3.56 kT/e$. The unit cell parameters are $a_x = a_y = 100$ Å while the patch has dimensions $b_x = b_y = 75$ Å and $\cos(\mathbf{k}\cdot\mathbf{d}) = -1$. The van der Waals interaction using a Hamaker constant of 2.2×10^{-20} J is given by the dotted line.

to a decay length of 30.5 Å which is definitely not the Debye length κ^{-1} ($=640.7$ Å), but is very close to $k_{\min}^{-1} = a/\pi = 31.8$ Å, indicating that an approximation by the asymptotic form that can be obtained from eq 32 would appear to be adequate when the separation exceeds about 75 Å for our choice of parameters.

In Figure 3 we demonstrate the dependence of the decay length on the salt concentration, with square lattices and square patch parameters of $a = 100$ Å, $b = 75$ Å, $\mathbf{d} = (100,100)$, $\Psi_0 = -75$ mV, and $\Psi_p = 133$ mV. Increasing the salt concentration by 2 orders of magnitude from $\kappa^{-1} = 640.7$ Å to $\kappa^{-1} = 64.1$ Å has little overall effect on the observed decay length. Not until the concentration is such that κ^{-1} is smaller than the smallest nonzero k^{-1} does the value of the decay length become close to the Debye length. With an increase of another 2 orders of magnitude in the salt concentration, to $\kappa^{-1} = 6.4$ Å, we finally see the decay length being determined by κ^{-1} .

In Figure 4 we show a comparison of the forces between constant potential and between constant charge surfaces, under identical geometrical parameters. It is important to note that a rectangular patch of *potential* strength, Ψ_p , as described by eq 36, does not produce a rectangular patch of *charge* strength, $\sigma_p = \epsilon_2 \kappa \Psi_p / 4\pi$, that can also be described by eq 36. In order to get the *charge* distribution corresponding to a given distribution of *potential* strength, one must use eq 15 appropriate to an isolated surface

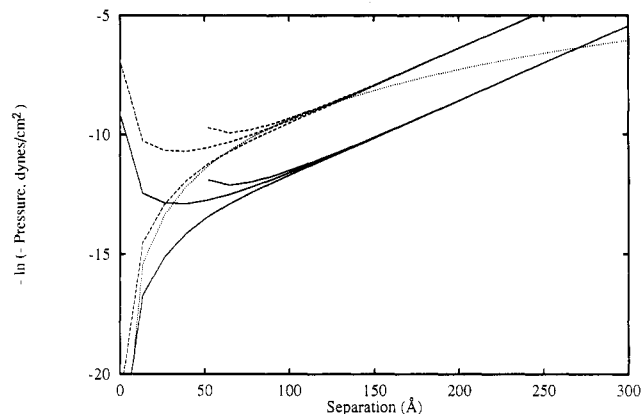


Figure 5. A comparison of equations of state for different potential strengths: the pressure vs surface separation for constant potential surfaces, constant charge with no dielectric discontinuities, and constant charge with dielectric discontinuities, $\epsilon_1 = \epsilon_3 = 2$. The underlying surface potentials were set at -25 mV (dashed lines) and -75 mV (solid lines) or -1 and $-3 kT/e$ and the potential on the patches was set accordingly at 3.56 and $5.33 kT/e$. The unit cell parameters are $a_x = a_y = 100$ Å while the patch has dimensions $b_x = b_y = 75$ Å and $\cos(\mathbf{k}\cdot\mathbf{d}) = -1$. The van der Waals interaction using a Hamaker constant of 2.2×10^{-20} J, is given by the dotted line.

to calculate the resulting charge distribution. This gives rise to another Fourier expansion for a spatially varying surface charge density which is different to the one described by eq 36. Thus when we speak of a constant charge interaction, we refer to that case in which the two-dimensional charge distribution is derived from the given potential distribution on an isolated surface and then this charge distribution is held constant as the two surfaces are brought together. In this manner, the constant charge and constant potential interactions will coincide at large separations. A comparison of a constant potential interaction and a constant charge interaction as described here is shown in Figure 4. The two upward turning curves represent constant charge results, with (i) $\epsilon_2 = 78.5$, $\epsilon_1 = \epsilon_3 = 2$ or (ii) $\epsilon_1 = \epsilon_3 = \epsilon_2 = 78.5$, respectively, for the most and least repulsive of the curves. In the absence of dielectric discontinuities, case (ii), the repulsive image effects will be smaller and the disjoining pressure turns repulsive at smaller separations. But at large enough separations the results of both cases merge in with the constant potential case as expected. The effect of the strength of the potential and corresponding surface charge on the forces for these three cases is shown in Figure 5. Note that all these curves have been calculated with the two lattices displaced by $\mathbf{d} = (100,100)$, so that $\cos(\mathbf{k}\cdot\mathbf{d}) = -1$.

With Figure 6 we focus again on constant potential surfaces. This time we consider asymmetric systems where one surface has a periodic distribution, with the zero U_0 constraint, while the other surface had a uniform surface (nonpatchy) potential distribution (independent of ρ), that is, there are no patches. The curve shown in Figure 4 is reproduced here for comparison. When the potential on the patches on the right surface is set to zero, the surface retains, in this case, a uniform net negative potential of -50 mV. At large separations, this corresponds to eq 34a as the appropriate asymptotic form, with $k_{\min} = 0$ and $q_{\min} = \kappa$. In the full expression, eq 30, the terms proportional to the phase factor, $\cos(\mathbf{k}\cdot\mathbf{d})$, do not appear, nor do all the higher order terms involving the (zero) Fourier coefficients of the right surface. It is quite clear that what remains of the contribution from $k \neq 0$ terms are small compared with the $k = 0$, large separation, asymptotic form, until very small separations. The fact that the force for the asymmetric problem is *more attractive* than the symmetric case may seem astounding at first, but that double layer attractions do arise for asymmetric surfaces behaving at constant potential has been seen before. It just so happens that with the Debye length being so large in this case, compared to $a/\pi = 31.8$ Å, the uniform term has not had a chance to decay

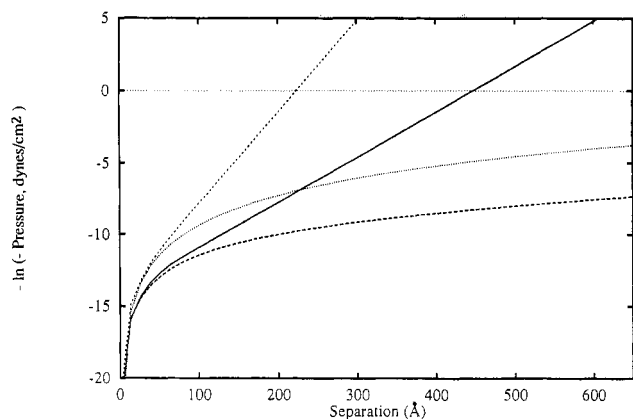


Figure 6. A comparison of the symmetric problem with two asymmetric problems for constant potential surfaces: the pressure vs surface separation for two nonuniform but overall neutral surfaces (solid line), one nonuniform overall neutral surface interacting a uniform charged surface with potential of -50 mV (long dashed line), and a nonuniform surface interacting with a uniform neutral surface (short dashed line). The parameters for the nonuniform neutral surfaces are an underlying surface potential of -50 mV or $-2 kT/e$, a patch potential of $3.56 kT/e$; unit cell parameters are $a_x = a_y = 100$ Å while the patch has dimensions $b_x = b_y = 75$ Å. The van der Waals interaction using a Hamaker constant of 2.2×10^{-20} J is given by the dotted line.

significantly. We should point out that the ordinate of the plot extends only out to about one Debye length, $\kappa^{-1} = 640.7$ Å. Consequently, although this force decays, according to (34a), exponentially over a distance of one-half this value, its true exponential form is not yet evident, and the force still shows some residual curvature.

If now the uniform potential on the uniform (nonpatchy) surface is also set to zero, we have the situation of one genuinely neutral surface interacting with a surface which is net neutral. Equation 34b is representative of this case with $k_{\min} = \pi/a$, and magnitude governed by the potential strength on the patches on the left surface which carries a periodic charge distribution. The change in the slope of the curve from $1/q_{\min}$ to $1/2q_{\min}$ is quite evident here. Incidentally, it is precisely this full profile which represents the difference between the uniform asymptotic result of the last case ($\Psi_0^R = -50$ mV) and the corresponding complete solution.

In Figure 7, we show the effects of increasing the unit cell size from a square of size 200 Å \times 200 Å to a square of size 400 Å \times 400 Å; the patch size is increased proportionally to maintain the same value of potentials everywhere. Naturally, the most significant effect is to double the decay length of the asymptotic exponential force. Comparisons of constant potential with constant charge, both with and without dielectric discontinuities, show that the curves begin to diverge at larger separations as the cell size is increased. The forces at constant charge also change from attractive to repulsive at larger separations. We should add two remarks here about calculations which we have performed but not presented. Firstly, instead of increasing the size of the patch, keeping the potentials constant, we could have kept the same patch size as before and either increased the patch potential by an appropriate amount, or lowered the value of the uniform background. The former process produces much larger forces than the result shown here, heading in the direction demonstrated in Figures 2 and 5. The latter process produces a force which is slightly less in magnitude than the one shown here. The second remark is that with square lattices, there are actually four contributions to the value of k_{\min} ; these come from the two combinations $(\pm 1, 0)$ and $(0, \pm 1)$, for the integers n and m defined in the paragraphs preceding eq 36. Consequently, four terms, equivalent to eqs 32–35, contribute, a situation which does not arise for rectangular systems. For example, if we were to instead increase the size of the square unit cell to a rectangular cell of dimensions 200 Å \times 400 Å, the patch changing proportionally,

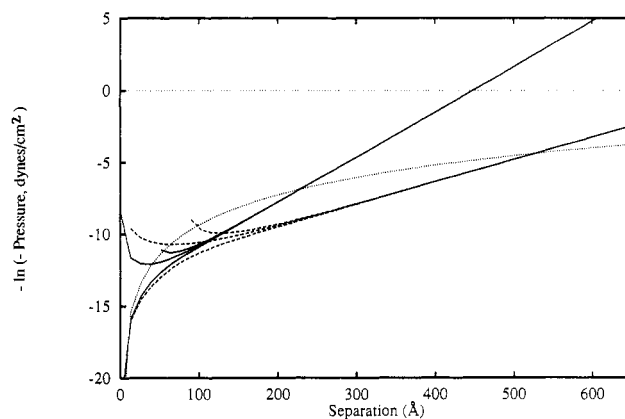


Figure 7. A comparison of equations of state for two unit cell sizes. The underlying surface potential was kept fixed at -50 mV or $-2 kT/e$ and the potential on the patches was $3.56 kT/e$. The pressures for surfaces of constant potential, constant charge with no dielectric discontinuities, and constant charge with dielectric discontinuities, $\epsilon_1 = \epsilon_3 = 2$, are grouped. For the upper grouping of forces (solid lines), the unit cell parameters are $a_x = a_y = 100$ Å with patches of dimensions $b_x = b_y = 75$ Å. For the lower grouping (dashed lines), the parameters are $a_x = a_y = 200$ Å and $b_x = b_y = 150$ Å. The salt concentration is 2.5×10^{-5} M. The van der Waals interaction using a Hamaker constant of 2.2×10^{-20} J is given by the dotted line. In both cases, $\cos(\mathbf{k} \cdot \mathbf{d}) = -1$.

the force would have the same decay as the one shown in the figure, $\sim 200/\pi$ Å, but with magnitude reduced by a factor of 2.

Finally, it is necessary to discuss some of the implications of the phase factor, $\phi = \cos(\mathbf{k} \cdot \mathbf{d})$, which arise in situations involving two interacting lattices. Firstly, we show in Figures 8 results for the extreme cases where the lattices are in register ($\phi = 1$) or are exactly out of register ($\phi = -1$), for symmetric neutral surfaces and for two square unit cell sizes. Both disjoining pressure (Figure 8a) and interaction potential (Figure 8b) are shown. There is little need for additional comment, except to say that despite the similar effects on both the pressure and the free energy, the pressure appears most sensitive to variations of either ϕ or cell size. In the next section, we consider the correct approach of obtaining a physically meaningful average with respect to this phase factor.

V. Average over Transverse Displacements

In terms of physically realistic experiments employing, for example, the surface force apparatus, the results quoted above for a well-defined lattice displacement could be considered relevant to the interaction of two rigid mica surfaces chemically modified with, say, ionizing radiation. For systems involving species adsorption, with which we are mostly concerned and which are most common experimentally, further considerations arise. We assume that on each surface the inhomogeneities retain their size and periodic distribution, but are otherwise allowed to migrate collectively on the surface. All other things being equal, the minimum energy configuration at any fixed separation occurs when the surface distributions migrate out of register. Intuitively, we would believe that the surfaces, initially uncorrelated and therefore in random relative displacement at infinite separation, would become correlated on approach in order for the system to minimize the free energy. This could conceivably occur provided that the time for the approach of the surfaces is sufficiently slow compared with the migration time on the surface. For this situation it is appropriate to then average, at a given h , over all possible relative displacements. As Richmond understood,⁴ the probability of the surfaces being aligned in high-energy configurations, relative to the probability of being in the low-energy configurations will be small. The behavior of a system would favor the low-energy configurations. Actually, the task which

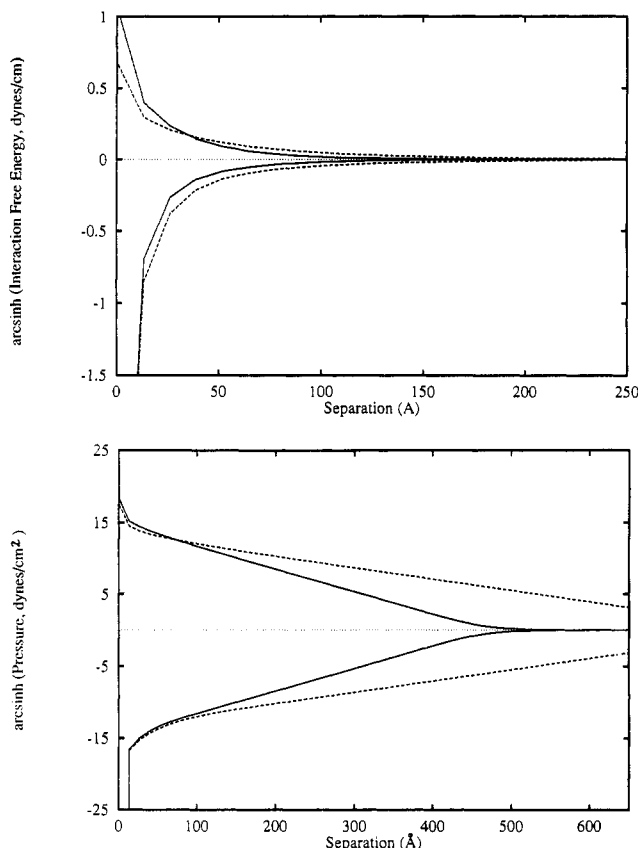


Figure 8. A comparison of relative displacement of surfaces at constant potential. The force and the interaction free energy per unit area are plotted on an arcsinh vertical scale. Two sets of unit cell parameters are used; these are $a_x = a_y = 100$ Å with patches of dimensions $b_x = b_y = 75$ Å (solid lines) and $a_x = a_y = 200$ Å with patches of dimensions $b_x = b_y = 150$ Å (dashed lines). The underlying surface potential was kept fixed at -50 mV or $-2 kT/e$ and the potential on the patches was $3.56 kT/e$; the surfaces are overall neutral. Part a (top) shows the disjoining pressure while part b (bottom) shows the interaction free energy per unit area. The interaction is most repulsive when and $\cos(\mathbf{k}\cdot\mathbf{d}) = 1$ and is most attractive when and $\cos(\mathbf{k}\cdot\mathbf{d}) = -1$.

should be considered is to calculate a partition function for the system, summing over all probabilities weighted by the free energy, $V(\mathbf{h}; \mathbf{d})$, of either form (30) or (31), associated with a given value of the relative lattice displacement, \mathbf{d} , on the two surfaces. In fact, we shall measure the probability in terms of the surfaces tangentially displaced with vector, \mathbf{d} , relative to the surfaces in the minimum energy configuration:

$$\delta V(\mathbf{h}; \mathbf{d}) = V(\mathbf{h}; \mathbf{d}) - V(\mathbf{h}; \cos(\mathbf{k}\cdot\mathbf{d}) = -1),$$

$$\exp(-\beta A \delta G(\mathbf{h})) = \frac{1}{A} \int \int_A \exp(-\beta A \delta V(\mathbf{h}; \mathbf{d})) \, d\mathbf{d} \quad (40)$$

where $A\delta G(\mathbf{h}) = A[G(\mathbf{h}) - V(\mathbf{h}; \cos(\mathbf{k}\cdot\mathbf{d}) = -1)]$ is the appropriate thermodynamic potential for a unit cell of surface area, A , relative to the minimum energy configuration. We point out that this procedure is *not* equivalent to simply averaging the interaction free energy given by eqs 30 and 31 over \mathbf{d} . Indeed such a step would be incorrect in that it eliminates all the contributions from the dominant asymptotic terms given by eqs 32 and 33.

Regrettably, it is not possible to perform the integration indicated in eq 40 analytically, using the full $V(\mathbf{h}; \mathbf{d})$. We have some reprieve from this dilemma, though, if we only wish to consider the behavior of $\delta G(\mathbf{h})$ at large separations. That is, if we replace the complete expression for $V(\mathbf{h})$ with its corresponding asymptotic form, eqs 32 or 33; for these cases the integral in eq 40 is tractable. Note that terms independent of \mathbf{d} in $V(\mathbf{h}; \mathbf{d})$ can be removed from under the integral sign.

Recall first that for rectangular lattices there are two terms contributing to leading order, each with a twofold degeneracy.

Let us write the reciprocal wave vectors for these cases as $\mathbf{k}_{10} = (\pi/a_x, 0)$ and $\mathbf{k}_{01} = (0, \pi/a_y)$. Both eqs 32 and 33 can then be written in the reduced form

$$V(\mathbf{h}) = \Omega_{10}(h) \cos(\mathbf{k}_{10}\cdot\mathbf{d}) + \Omega_{01}(h) \cos(\mathbf{k}_{01}\cdot\mathbf{d}) \quad (41)$$

where the meaning of the coefficients should be obvious from eqs 32 and 33, apart from an implicit factor of 2 which accounts for the twofold degeneracy. Since the function $V(\mathbf{h}; \cos(\mathbf{k}\cdot\mathbf{d}) = -1)$ is independent of \mathbf{d} , we only need to consider the terms $G(\mathbf{h})$ and $V(\mathbf{h}; \mathbf{d})$ in eq 40. The integration can be written explicitly as

$$\begin{aligned} \exp(-\beta A G(\mathbf{h})) &= \frac{1}{A} \int \int ds \exp(-\beta(A\Omega_{10}(h) \cos(\pi x/a_x) + \\ &\quad A\Omega_{01}(h) \cos(\pi y/a_y))) \quad (42) \\ &= \frac{1}{A} \int_{-a_x}^{a_x} dx \exp(-\beta A\Omega_{10}(h) \cos(\pi x/a_x)) \int_{-a_y}^{a_y} dy \times \\ &\quad \exp(-\beta A\Omega_{01}(h) \cos(\pi y/a_y)) \end{aligned}$$

However, these are just integral representations of the modified Bessel function of the first kind with order zero given by $I_0(v)^{10}$

$$I_0(v) = \frac{1}{2\pi} \int_0^{2\pi} e^{v \cos(u)} \, du \quad (43)$$

with $v = \beta A\Omega_{10}$ or $\beta A\Omega_{01}$. Consequently, we arrive at the asymptotic form for the free energy per unit area, $G(\mathbf{h})$, that had been averaged over all transverse displacements

$$G(\mathbf{h}) = -\frac{kT}{A} \ln(I_0(\beta A\Omega_{10}(h))I_0(\beta A\Omega_{01}(h))) \quad (44)$$

Since the modified Bessel function, I_0 , is always positive and is a monotonically increasing function, this displacement-averaged free energy is always negative. That is, the average interaction free energy of surfaces arising from the presence of charged patches on the surfaces is always attractive. This is independent of whether the surfaces are held at constant charge or constant potential. It is also independent of whether we have a symmetric system or an antisymmetric potential system (when the potential on the patches on one surface is opposite to that on the other). We should also add that the arguments leading to eq 44 are valid for any lattice. In the case where the lattice is rectangular, only one of the Bessel functions should appear corresponding to the larger of a_x or a_y , although both can be included without additional effort. Although it is incidental to our interest, we remark that one can repeat the above analysis to evaluate the average energy (see the Appendix).

Further information can be gleaned from the asymptotic form of displacement-averaged interaction free energy, $G(\mathbf{h})$, as a function of separation. At very large separations, the arguments of the modified Bessel functions are exponentially small, and we can consider a small argument expansion of the I_0 's. Multiplying the two I_0 terms and expanding the natural logarithm leads to the following asymptotic dependence on separation, for square lattices ($a_x = a_y = a$)

$$G(\mathbf{h}) = -\frac{A}{kT} \Omega^2 \exp(-2q_{\min}h) \quad (45)$$

where $q_{\min} = [(\pi/a)^2 + \kappa^2]^{1/2}$ and the constant Ω can be found from eqs 41 and either eq 32 for constant potential or eqs 33 for constant charge. A number of important features of G should be emphasized. The attractive force between correlated net neutral surfaces decays exponentially with decay length, $(2q_{\min})^{-1}$, which is one-half that found for surfaces held in the optimal configuration. Given the above asymptotic form of G , we can see that when the salt concentration is low $q_{\min} \approx \kappa_{\min}$ and the decay is again determined by the lattice spacing. Also, from (32) and

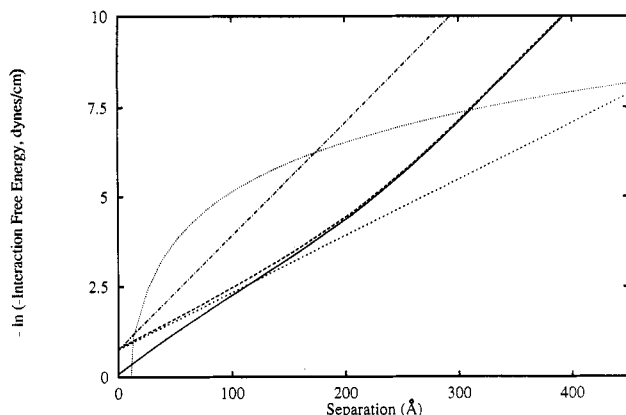


Figure 9. A comparison of the thermodynamic averaged interaction free energy, $G(h)$ (long dashed line), with the unaveraged contribution, eq 32 (short dashed line) and the leading, \mathbf{d} -independent contribution, eq 46a (dot-dashed line). The sum of G and eq 46a (solid line) is given for comparison with van der Waals (dotted line). These have been calculated assuming a base potential of -75 mV or $-3 kT/e$ and a patch potential of $5.3 kT/e$. The lattice has a unit cell of size $a_x = a_y = 200$ Å and the patch has dimensions $b_x = b_y = 150$ Å.

(33), the magnitude of the interaction potential, G , depends inversely on temperature; that is, it decreases linearly as the temperature increases. No strong dependence on salt concentration is expected. When the salt concentration is high, that is when $q_{\min} \approx \kappa$, the decay is half the inverse Debye length, $(2\kappa)^{-1}$. For constant potential surfaces the magnitude depends inversely on the temperature squared and is proportional to salt concentration. For constant charge surfaces with low dielectric half spaces, the average interaction potential has no direct dependence on temperature and is inversely dependent on concentration. These dependences suggest a number of experiments which could be performed for confirmation.

Since the separation dependence of G is, to leading order, identical to the first nonvanishing, \mathbf{d} -independent term of eqs 30 and 31, respectively, they should be included together for consistency. That is, to obtain the leading asymptotic form for the interaction free energy, $G(h)$ above should be added to terms in eq 46 for each of the degenerate contributions of k_{\min} . For constant potential surfaces we add to G the attractive term

$$V^P(h) = -\frac{\epsilon_2 q_{\min}}{4\pi} (\Psi_{-\mathbf{k}}^L \Psi_{\mathbf{k}}^L + \Psi_{-\mathbf{k}}^R \Psi_{\mathbf{k}}^R)_{k=k_{\min}} \exp(-2q_{\min} h) \quad (46a)$$

For constant charge surfaces one must add the repulsive term

$$V^C(h) = 4\pi\epsilon_2 q_{\min} \left(\frac{\sigma_{-\mathbf{k}}^L \sigma_{\mathbf{k}}^L \Delta_{23}}{(\epsilon_2 q + \epsilon_1 k)^2} + \frac{\sigma_{-\mathbf{k}}^R \sigma_{\mathbf{k}}^R \Delta_{21}}{(\epsilon_2 q + \epsilon_3 k)^2} \right)_{k=k_{\min}} \times \exp(-2q_{\min} h) \quad (46b)$$

In Figure 9 we compare $G(h)$ of (44) alone with the asymptotic expression for the interaction potential between net neutral surfaces in the minimum energy configuration, given by eq 32, and with the expression given by eq 46a. We also include the profile for the sum of $G(h)$ and (46a), as well as the familiar van der Waals interaction energy. Only the constant potential case is considered.

VI. Conclusions

The importance effects of heterogeneous surface charges had been considered in earlier work. Vreeker et al.¹¹ had considered the effect of a heterogeneous surface modeled as a surface with a two-dimensional sinusoidal variation in the surface potential. With the simplified treatment of Kuin,⁶ they showed that with

reasonable parameter values for the sinusoidal component of the surface potential they can fit the observed variations in the coagulation stability ratio of nickel hydroxycarbonate particles with indifferent electrolyte concentration. Burnham et al.¹² also suggested that surface heterogeneity can also arise due to work function variations along the surface that can give rise to charged patches on an otherwise net neutral surface. Estimates of the electrostatic interaction of two such surfaces across an air gap had been put forward as the explanation of long-ranged attractions observed in force microscopy. Therefore, it appears that effects due to surface heterogeneities require further study and investigation in order for us to evaluate its quantitative impact on the theoretical notions of colloidal stability and particle interactions. This paper is a first step in this direction.

We have considered in some detail the interaction between surfaces whose sources of charge or potential are nonuniformly distributed. Full analytical detail is given for the general case of two completely dissimilar surfaces with periodically distributed sources. Numerical and asymptotic results are given for the special case when the surfaces have identical periodic lattice structure. These results show that when the surfaces are net neutral there remains a substantial interaction which decays exponentially with separation between the surfaces. Both the magnitude and sign and the characteristic decay length of the interaction are dependent on whether the surface is held at constant charge or constant potential and on the relative displacement of the lattices. The main findings of this paper obtained within the Debye-Hückel treatment are as follows:

1. For net neutral surfaces that contain periodic charge distributions, a net interaction exists whose magnitude is governed by the strength of the periodic sources, and the underlying uniform charge distribution does not play any role apart from providing a neutral surface.

2. The interaction decays exponentially with the decay length controlled by the periodicity of the charge inhomogeneities and the Debye length κ^{-1} . If the Debye length is large, i.e., low salt concentrations, this characteristic decay length is dictated by the lattice spacing; at high salt (small Debye length), the decay is determined by κ^{-1} .

3. The extra interaction associated with charge inhomogeneities can be attractive or repulsive depending on the relative transverse displacement of the periodic charge distribution.

4. For the case when the surface charge distributions are free to migrate to lower the interaction free energy, a full statistical mechanical average shows that the leading term is always attractive irrespective of the nature of the surface.

The above results should be taken into account in any attempt to interpret measured forces between mica surfaces which have been modified with adsorbed or deposited ionic surfactants in terms of hydrophobic effects.

Appendix

Kuin⁶ gave results for the thermodynamically averaged interaction potential, $E(h)$, defined as

$$E(h) = \langle V(h; \mathbf{d}) \rangle_{\mathbf{d}} \equiv \frac{\frac{1}{A} \int \int_A V(h; \mathbf{d}) \exp(-\beta A \delta V(h; \mathbf{d})) \, \mathbf{d}\mathbf{d}}{\exp(-\beta A \delta G(h))} \quad (A1)$$

From this definition, Kuin derived an approximate functional form by using a Taylor series expansion for $V(h; \mathbf{d})$ about its minimum value which occurs in our case when the surfaces are out of register, that is $V(h; \cos(\mathbf{k} \cdot \mathbf{d}) = -1)$. Since Kuin used the superposition approximation to obtain his V , his expression would, at best, only hold at large separations. However, this is precisely

the regime in which we were able to determine $G(h)$ of eq 40. Furthermore, the form given by (41) suggests that it would be equally straightforward to perform the integration in the numerator of eq A1. By expressing V as the sum of the \mathbf{d} -independent terms shown in eqs 46 and eq 41 we can show that (A1) simplifies to

$$E(h) = \frac{\int \int_A V(h; \mathbf{d}) \exp(-\beta A V(h; \mathbf{d})) d\mathbf{d}}{\int \int_A \exp(-\beta A V(h)) d\mathbf{d}} + V(h; \mathbf{d}\text{-independent})$$

$$= \frac{\Omega_{10}(h) \int_{-a_x}^{a_x} dx \cos(\pi x/a_x) \exp(-\beta A \Omega_{10}(h) \cos(\pi x/a_x))}{I_0(\beta A \Omega_{10}(h))} + \frac{\Omega_{01}(h) \int_{-a_y}^{a_y} dy \cos(\pi y/a_y) \exp(-\beta A \Omega_{01}(h) \cos(\pi y/a_y))}{I_0(\beta A \Omega_{01}(h))} + V(h; \mathbf{d}\text{-independent}) \quad (\text{A2})$$

The remaining integrals are, of course, just the modified Bessel functions of first order, $I_1(x)$.¹⁰ The asymptotic form for $E(h)$

is then given by

$$E(h) = \frac{\Omega_{10}(h) I_1(\beta A \Omega_{10}(h))}{I_0(\beta A \Omega_{10}(h))} + \frac{\Omega_{01}(h) I_1(\beta A \Omega_{01}(h))}{I_0(\beta A \Omega_{01}(h))} + V(h; \mathbf{d}\text{-independent}) \quad (\text{A3})$$

References and Notes

- (1) Verwey, E. J. W.; Overbeek, J. Th. G. *Theory of the Stability of Lyophobic Colloids*; Elsevier: New York, 1948.
- (2) Carnie, S. L.; Torrie, G. *Adv. Chem. Phys.* **1984**, *56*, 141.
- (3) Pashley, R. M.; McGuiggan, P. M.; Ninham, B. W.; Evans, D. F. *Science* **1985**, *229*, 1088.
- (4) Richmond, P. (a) *J. Chem. Soc., Faraday Trans. 2* **1974**, *70*, 1066; (b) *J. Chem. Soc., Faraday Trans. 2* **1975**, *71*, 1154.
- (5) Nelson, A. P.; McQuarrie, D. A. *J. Theor. Biol.* **1975**, *55*, 13.
- (6) Kuin, A. J. *Faraday Discuss. Chem. Soc.* **1990**, *90*, 235.
- (7) Chan, D. Y. C.; Mitchell, D. J. *J. Colloid Interface Sci.* **1983**, *95*, 193.
- (8) Chan, D. Y. C. In *Geochemical Processes at Mineral Surfaces*; Davis, J. A., Hayes, K. F., Eds.; ACS Symposium Series, No. 323; American Chemical Society: Washington, DC, 1986; p 99.
- (9) Israelachvili, J. I.; Adams, G. E. *J. Chem. Soc., Faraday Trans. 1* **1978**, *74*, 975.
- (10) Morse, P. M.; Feshbach, H. *Methods of Theoretical Physics*; McGraw-Hill: New York, 1953; Vol. II.
- (11) Vreeker, R.; Kuin, A. J.; den Boer, D. C.; Hoekstra, L. L.; Agerof, W. G. M. *J. Colloid Interface Sci.* **1992**, *154*, 138.
- (12) Burnham, N. A.; Colton, R. J.; Pollock, H. M. *Phys. Rev. Lett.* **1992**, *69*, 144.